to be observed. The nitrogen nuclei, mainly ^{14}N with 0.4036 nuclear magnetons and spin value 1, also would not produce appreciable nuclear specific heat at this temperature range even with a megagauss exchange field, and exchange fields of this magnitude in the vicinity of the nitrogen nuclei are very unlikely, since a pronounced p character of the electronic wave functions is expected in this region.

In summary, our experiments on uranium nitride have shown specific heats in the 1.3–4.7°K temperature range consist only of a large electronic term γT and a lattice specific heat characterized by $\Theta=322$–326°K with little or no magnetic specific heat. Evidently actinide compounds, like uranium nitride, have higher γ than similar transition-metal compounds or the rare-earth metals because of the $5f$ states near the Fermi surface, whereas in the rare-earth metals the narrow $4f$ electron band is well removed from the Fermi surface and in the transition-metal compounds the f bands are not present and the d bands are relatively broad. A complete resolution of the factors that cause the enhancement of the density of electronic states of uranium nitride, i.e., narrowing of the $5f$ band, electron-phonon, or exchange enhancement, remains uncertain since we cannot separate them solely by specific-heat measurements. Finally, the higher Debye temperature obtained from our measurements has removed any necessity of detailed explanations for an abnormally small entropy of magnetic ordering, which appears only to be due to misinterpretation of previous specific-heat data.

PHYSICAL REVIEW VOLUME 176, NUMBER 2 10 DECEMBER 1968

High-Field Galvanomagnetic Effects in Antiferromagnetic Chromium*†

A. J. ARKO‡ AND J. A. MARCUS
Northwestern University, Evanston, Illinois§
AND
W. A. REED
Bell Telephone Laboratories, Murray Hill, New Jersey

(Received 22 July 1968)

The effects of the antiferromagnetic spin-density wave on the Fermi surface of Cr have been investigated by measurement of the high-field galvanomagnetic properties of pure single-domain crystals of Cr (residual resistance ratios from 750 to 1760) in fields up to 200 kOe. The topological features of the Fermi surface are shown to be consistent with a single direction of open orbits parallel to **Q**, the wave vector of the spin-density wave, in agreement with the Lomer model of the Fermi surface. Magnetic breakdown through the superlattice energy gaps is observed in the 0–20-kOe range and again in the 60–200-kOe range for all orientations of **H**. Theoretical calculations by Falicov and Zuckermann suggest that the breakdown is probably occurring through the second- and first-order gaps. An estimate of the breakdown fields is made by comparing our results with the theoretical curves of Falicov and Sievert. The value of the energy gaps depends sensitively on the type of energy bands assumed, but a lower bound for first-order gaps is ~0.05 eV. Measurements on multidomain crystals and the effects of a compressive stress are also discussed.

I. INTRODUCTION

IN a metal the effect of a periodic potential of wave vector $\mathbf{q}$ is to mix electronic states belonging to $\mathbf{k}$ with those belonging to $\mathbf{k}'=\mathbf{k}\pm\mathbf{q}$. Gaps appear in the energy spectrum at $\mathbf{k}$ and $\mathbf{k}'$ when the energy $E(\mathbf{k})=E(\mathbf{k}')$. For the periodic potential due to the crystal lattice, energy gaps occur along planes which define the Brillouin zones.

The periodic potential associated with antiferromagnetic ordering of the sort that has been invoked to account for the unique properties of Cr results in energy gaps that drastically change the topology of the Fermi surface.[1–3] The purpose of the present work is to investigate the effect of antiferromagnetic ordering on the topology of the Fermi surface of Cr by measuring the high-field galvanomagnetic properties[4] of single-domain single crystals.

* This paper is based in part on a dissertation submitted to Northwestern University by A. J. Arko in partial fulfillment of the requirements for the degree of Doctor of Philosophy.

† Part of this work was performed while the authors were guest scientists at the Francis Bitter National Magnet Laboratory which is supported at MIT by the Air Force Office of Scientific Research.

‡ Present address: Argonne National Laboratory, Argonne, Ill.

§ Supported by the National Science Foundation and the Advanced Research Project Agency of the Department of Defense, through the Materials Research Center of Northwestern University.

[1] W. M. Lomer, in *Proceedings of the International Conference on Magnetism, Nottingham, 1964* (Institute of Physics and The Physical Society, London, 1965), p. 127.

[2] L. M. Falicov and M. J. Zuckermann, Phys. Rev. **160**, 372 (1967).

[3] A. W. Overhauser, Phys. Rev. **128**, 1437 (1962).

[4] By "high-field" we mean $\omega_c\bar{\tau}\gg 1$ for all carriers where ω_c is the cyclotron frequency eH/m^*c, and $\bar{\tau}$ is the relaxation time averaged over the orbit.

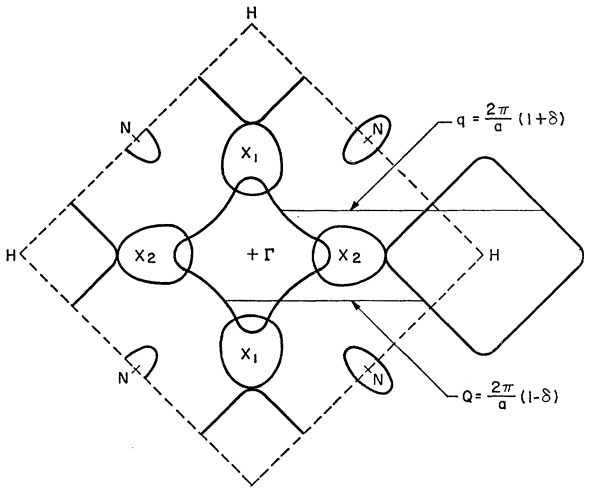

FIG. 1. ⟨100⟩ cross section of the paramagnetic Fermi surface of Cr as proposed by Lomer (Ref. 11), showing the superlattice wave vector **Q**, and the vector $\mathbf{q}=(2\pi/a)\,[200]-\mathbf{Q}$.

Neutron diffraction experiments[5–10] have established that in the antiferromagnetic phase the magnetic moment of the electron spins at corner sites of the Cr bcc lattice is antiparallel but not quite equal to the magnetic moment at the body-centered sites. The amplitude of the moment is sinusoidally modulated with a wavelength a/δ, where a is the lattice constant and δ is a dimensionless quantity that varies from ~ 0.035 at the Néel temperature ($T_N=312$°K) to ~ 0.05 at 4.2°K. The structure has been described as a linear spin-density wave[3] with a fundamental wave vector, $\mathbf{Q}=(2\pi/a)(1-\delta, 0, 0)$. The spin-density wave is stabilized by an interaction[11,12] between two large pieces of the Fermi surface centered at Γ and H (see Fig. 1) that have large, flat, almost parallel surfaces separated by **Q**. The fundamental spin-polarization wave is modulated by the crystal lattice so that the spin-density wave is composed of all waves having wave vectors

$$\mathbf{q}=\mathbf{G}\pm\mathbf{Q}, \tag{1}$$

where $\{\mathbf{G}\}$ is the set of reciprocal lattice vectors.

Montalvo and Marcus[13] discovered that cooling a crystal of Cr through T_N in a magnetic field, $H_c>20$ kOe, applied along a ⟨100⟩ axis changes the symmetry of phenomena associated with the Fermi surface from cubic to tetragonal, with the tetragonal axis parallel to H_c. To interpret the magnetic anisotropy data, Lomer and Marcus[14] assumed a domain model that, however, was unable to distinguish between a tetragonal state consisting of an equal mixture of **Q**'s perpendicular to $\mathbf{H}_c$, or a single **Q** parallel to $\mathbf{H}_c$. Watts[15] concluded that only $\mathbf{Q}\parallel\mathbf{H}_c$ could account for the complete tetragonality of his preliminary high pulsed-field de Haas–van Alphen (dHvA) data. Subsequent neutron diffraction experiments[16,17] verified that while in an untreated crystal there is generally a distribution of **Q**'s along the three cubic axes, the effect of cooling in a field is to produce a single-**Q** state, with $\mathbf{Q}\parallel\mathbf{H}_c$. From dHvA data, Graebner and Marcus[18] established that the apparently cubic state of Cr is a multidomain state, each domain containing a single **Q**. The ability to orient **Q**, and hence the tetragonal axis of the Fermi surface of Cr, along any of three mutually perpendicular directions makes Cr unique among metals.

The model of the Fermi surface of Cr as modified by the antiferromagnetic superlattice energy gaps has been discussed by Lomer[1] and Falicov and Zuckermann.[2] The most significant feature (discussed in detail in Sec. II) is the prediction of open electron trajectories. Since high-field galvanomagnetic phenomena are directly related to the topology of the Fermi surface, they are the most direct means of verifying the model.

The results of the Lifschitz, Azbel', and Kaganov[19] (LAK) theory of high-field galvanomagnetic effects are summarized in Sec. III and the experimental details are discussed in Sec. IV. The data presented in Sec. V consist only of measurements on single-domain crystals. Phenomena associated with multidomain measurements, including the effects of stress, are discussed in the Appendix. The discussion in Sec. VI is presented in two parts. In VI A the topological features of the Fermi surface are determined from the data in terms of the LAK theory. In VI B deviations of the magnetoresistance from the ideal quadratic behavior predicted by the LAK theory are interpreted in terms of magnetic breakdown through the superlattice energy gaps, as reported in a preliminary communication.[20] A rough estimate of the magnitude of the gaps is obtained using the calculations of Falicov and Sievert[21] and those of

[5] C. G. Shull and M. K. Wilkinson, Rev. Mod. Phys. **25**, 100 (1953).
[6] L. M. Corliss, J. M. Hastings, and R. J. Weiss, Phys. Rev. Letters **3**, 211 (1959).
[7] V. N. Bykov, V. S. Golovkin, N. V. Ageev, V. A. Levdik, and S. I. Vinogradov, Dokl. Akad. Nauk USSR **128**, 1153 (1959) [English transl.: Soviet Phys.—Doklady **4**, 1070 (1959)].
[8] G. E. Bacon, Acta Cryst. **14**, 823 (1961).
[9] G. Shirane and W. J. Takei, J. Phys. Soc. Japan Suppl. **17**, 35 (1962).
[10] Y. Hamaguchi, E. O. Wollan, and W. C. Koehler, Phys. Rev. **138**, A737 (1965).
[11] W. M. Lomer, Proc. Phys. Soc. (London) **80**, 489 (1962); **84**, 327 (1964).
[12] P. A. Fedders and P. C. Martin, Phys. Rev. **143**, 245 (1966).
[13] R. A. Montalvo and J. A. Marcus, Phys. Letters **8**, 151 (1964).
[14] W. M. Lomer and J. A. Marcus, in *Proceedings of the International Conference on Magnetism, Nottingham, 1964* (The Institute of Physics and The Physical Society, London, 1965), p. 208.
[15] B. R. Watts, Phys. Letters **10**, 275 (1964).
[16] A. Arrott, S. A. Werner, and H. Kendrick, Phys. Rev. Letters **14**, 1022 (1965).
[17] T. J. Bastow and R. Street, Phys. Rev. **141**, 510 (1966).
[18] J. E. Graebner and J. A. Marcus, J. Appl. Phys. **37**, 1262 (1966).
[19] I. M. Lifshitz, M. Ya. Azbel', and M. I. Kaganov, Zh. Eksperim. i Teor. Fiz. **31**, 63 (1956) [English transl.: Soviet Phys.—JETP **4**, 41 (1957)].
[20] A. J. Arko, J. A. Marcus, and W. A. Reed, Phys. Letters **23**, 617 (1966).
[21] L. M. Falicov and P. R. Sievert, Phys. Rev. **138**, A88 (1965).

Falicov and Zuckermann.[2] In some samples, a zero longitudinal magnetoresistive voltage was observed from 20 to 150 kOe, the highest field for which data were obtained. Some data showing this anomalous effect are presented in Sec. V, but the interpretation of the results in terms of geometrical effects, exaggerated by the anisotropy of the magnetoresitance, will be reported in a separate paper.[22]

II. FERMI SURFACE OF CHROMIUM

Figure 1 shows a ⟨100⟩ cross section of the Fermi surface of "paramagnetic" Cr as proposed by Lomer.[1] The surfaces centered at H and N are closed hole surfaces while the remaining are closed electron surfaces.

Lomer[1] and Falicov and Zuckermann[2] treated the effect of the antiferromagnetic superlattice as a perturbation of the crystal lattice problem. The effect of the perturbing spin-density wave potential is to mix electronic states belonging to $(\mathbf{k})$ with those belonging to $(\mathbf{k}+\mathbf{G}\pm\mathbf{Q})$ in the first order, with $(\mathbf{k}+\mathbf{G}\pm 2\mathbf{Q})$ in the second order, etc. At all points in the Brillouin zone satisfying the condition

$$E(\mathbf{k})=E(\mathbf{k}+\mathbf{G}\pm n\mathbf{Q}), \tag{2}$$

energy gaps occur in the nth order of the perturbation and an electron traveling on a constant energy contour will be Bragg diffracted at these energy gaps. In the extended zone scheme the condition for Bragg diffraction is given by

$$E(\mathbf{k})=E(\mathbf{k}\pm n\mathbf{Q}), \tag{3}$$

and the locus of points satisfying this condition defines the Bragg diffraction surface of the superlattice.

To map out the magnetic Bragg diffraction surfaces, various pieces of the Fermi surface are translated in the extended zone scheme by vectors $\pm n\mathbf{Q}$ and the locus of points of intersection with any other pieces of the Fermi surface determined. To show all the gaps in one zone it is necessary to translate by $\mathbf{G}\pm n\mathbf{Q}$. In Fig. 2 some of these translations are shown for the pieces at Γ, H, N and the pieces labeled X.

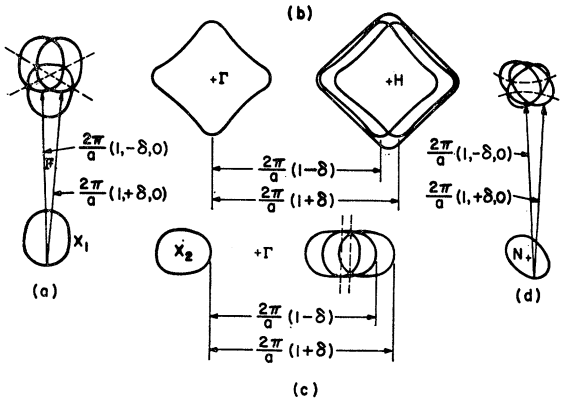

FIG. 2. Individual pieces of the Fermi surface translated by $(\mathbf{G}\pm\mathbf{Q})$. Dashed lines indicate the lines of intersection with other pieces of the Fermi surface and correspond to first-order energy gaps.

[22] A. J. Arko, J. A. Marcus, and W. A. Reed (to be published).

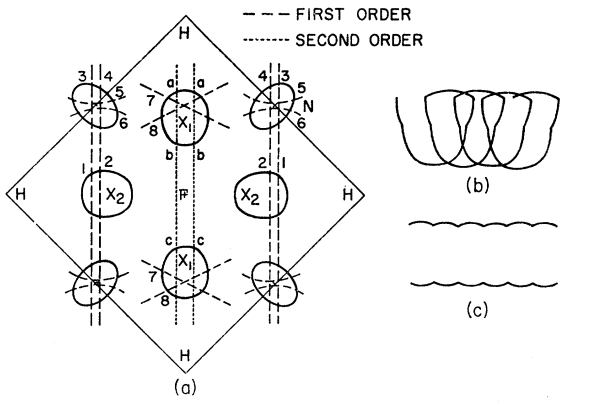

FIG. 3. (a) Intersections of the superlattice Bragg diffraction surfaces with the Fermi surface of Cr. Pieces at Γ and H are omitted. Points in k space connected in the first order are shown by identical numbers, points connected in the second order are shown by identical letters. (b) Typical open orbits due to first-order gaps on pieces labeled X_1. (c) Typical open orbits due to first-order gaps on pieces labeled X_2.

If the electron octahedron at Γ is translated by $\mathbf{Q}$ or by $(2\pi/a)(2,0,0)-\mathbf{Q}$ [Fig. 2(b)] its surface almost coincides with the surface of the hole octahedron at H. A first-order energy gap occurs along almost the entire region of coincidence, effectively eliminating these pieces from the Fermi surface. This is assumed to be the interaction that stabilizes the spin-density wave.

Some of the possible Bragg diffraction surfaces are shown[23] in Fig. 3(a). The pieces at Γ and H have been omitted, although a small hole surface centered at H probably remains after the interaction. Some of the open orbits that result from this modification of the Fermi surface are shown in Figs. 3(b) and 3(c). A great variety of orbits, both open and closed, are possible but no attempt will be made to describe them all. However, *all* of the open orbits predicted by this model are directed parallel to $\mathbf{Q}$.

III. SUMMARY OF HIGH-FIELD GALVANOMAGNETIC THEORY

In the high-field limit $(\omega_c\tau>1)$, the galvanomagnetic properties of metals are generally well understood. The LAK theory, together with the papers of Lifschitz and Peschanskii,[24] shows that the galvanomagnetic properties are determined solely by the state of compensation (the relative number of holes and electrons) and the topological features of the Fermi surface.[25]

[23] In constructing the antiferromagnetic Fermi surface we have included only the first- and second-order gaps. Falicov and Zuckermann (Ref. 2) have argued that for $H>1$ kOe, energy gaps of order three and higher have suffered complete magnetic breakdown and no longer affect the electron trajectories.

[24] I. M. Lifshitz and V. G. Peschanskii, Zh. Eksperim. i Teor. Fiz. **35**, 1251 (1958); **38**, 188 (1960) [English transls.: Soviet Phys.—JETP **8**, 875 (1959); **11**, 137 (1960)].

[25] For a review of the subject, see E. Fawcett, Advan. Phys. **13**, 139 (1964).

TABLE I. Field dependence of galvanomagnetic properties of metals at high fields.

Type of orbit and state of compensation	Transverse magnetoresistance	Hall voltage	Transverse-even voltage
All closed and uncompensated	Saturates	$\propto H$	Saturates
All closed and compensated	$\propto H^2$	$\propto H$	$\propto H^2$
Single open direction	$A+BH^2\cos^2\alpha$	$\propto H$	$BH^2\sin\alpha\cos\alpha$
Two or more open directions	Saturates	$\propto 1/H$	Saturates

The results of the LAK theory are summarized in Table I where the field dependence of the various galvanomagnetic properties is shown for a direction of **H** normal to the current **J**. The theory predicts saturation of $\Delta\rho/\rho$ for **H** || **J**, independent of topology. Case 3 is of particular interest in our investigation since it shows that for a single direction of open orbits making an angle α with **J**, the unique relationship between the magnetoresistive voltage and the transverse-even voltage leads to an unambiguous determination[26] of α.

While the relationships of Table I have been well substantiated in cases where the character of the electronic orbits remains constant in **H**, they do not necessarily apply if magnetic breakdown occurs. In the latter case the topology of the Fermi surface and/or the degree of compensation may change as **H** is increased. This may result in a change in the field dependence of magnetoresistance from quadratic to saturation or vice versa, depending on the details of the breakdown.

The term magnetic breakdown describes a situation where an electron, traveling on one sheet of the Fermi surface in the presence of a magnetic field, arrives at a Bragg diffraction surface, tunnels through the energy gap Δ, and continues its orbit on another sheet of the Fermi surface. The probability of tunneling depends on Δ and is given by the expression[27]

$$P=\exp(-H_0/H), \tag{4}$$

where, for free electrons, the characteristic breakdown field is given by

$$H_0=\pi\Delta^2/(4\hbar e\,|\,v_\perp v_{||}\,|). \tag{5}$$

In this equation $v_\perp$ and $v_{||}$ are the components of the *free-electron velocity* normal and parallel to the energy gap.

Another manifestation of magnetic breakdown is the occurrence of large-amplitude oscillations in the galvanomagnetic effects, periodic in $1/H$, with frequencies equal to the dHvA frequencies of the pieces undergoing magnetic breakdown.[28] This results from the modulation of the breakdown probability by the corresponding Landau levels. Pippard[29,30] has shown that the exact form of modulation depends critically on the particular network of orbits under consideration.

Falicov and Sievert[21] have calculated the effect of magnetic breakdown on the monotonic galvanomagnetic effects in metals. Although their calculations represent an idealized case of circular (free-electron) orbits, they nevertheless serve as a useful guide in interpreting data in Cr where the orbits are far from free-electron-like.

IV. EXPERIMENTAL DETAILS

The crystals, grown by thermal decomposition of chromium iodide, were obtained from Battelle Memorial Institute through the Chromalloy Corp. Only a very small percentage exhibited sufficient crystalline perfection to be useful in our measurements. Three of the crystals were oriented, using Laue back-reflection techniques and spark planed so that the specimen axis was within $\pm1°$ of the desired crystallographic axis. The surface damage was removed by electropolishing. Since the growth axis of most of the naturally occurring crystals was ⟨100⟩, it was possible to make some measurements on uncut crystals. The dimension of these crystals were of the order of 10 mm×3 mm×3 mm, although the cross section was not constant. Current and potential leads were spot-welded to the specimen except in some cases where they were soldered to minimize damage to the crystal. A description of the samples is given in Table II.

Measurements up to 32 kOe were made with an 11-in. iron-core electromagnet that could be rotated in the horizontal plane, together with a rotating probe capable of one degree of freedom. Measurements up to 200 kOe, carried out at the Francis Bitter National Magnet Laboratory, were made with a water-cooled solenoid and a rotating probe capable of two degrees of freedom.[31] The dc voltages were measured with a Keithley microvoltmeter and the data plotted on an *x-y* recorder.

Prior to making measurements the samples were cooled through T_N in fields up to 205 kOe to obtain a

[26] J. R. Klauder and J. E. Kunzler, Phys. Rev. Letters **6**, 179 (1961).
[27] E. I. Blount, Phys. Rev. **126**, 1636 (1962).
[28] R. W. Stark, Phys. Rev. Letters **9**, 482 (1962).
[29] A. B. Pippard, Proc. Roy. Soc. (London) **A270**, 1 (1962); Phil. Trans. Roy. Soc. (London) **A256**, 317 (1964); Proc. Roy. Soc. (London) **A287**, 165 (1965).
[30] L. M. Falicov, A. B. Pippard, and P. R. Sievert, Phys. Rev. **151**, 498 (1966).
[31] G. F. Brennert, W. A. Reed, and E. Fawcett, Rev. Sci. Instr. **36**, 1267 (1965).

TABLE II. Description of samples.

Sample	Direction of J	RRR with Q⊥J	RRR with Q not ⊥J	Dimensions in mm	Separation of magneto-resistance probes in mm	$R_{4.2°K}$ in $\mu\Omega$
Cr 1	[001]	740	•••	uncut	3	0.089
Cr 9	[001]	1030	750	0.9×1.27×7	2.4	0.281
Cr 10	[110]	1140	910	0.81×0.80×5	1.5	0.285
Cr 12	[001]	730	•••	1.65×1.50×8.2	2.4	0.16
Cr 256	[001]	1760	1310	uncut	•••	0.024
Cr 260	[001]	1560	•••	uncut	a. 4.8 b. 4.9	a. 0.09 b. 0.105

single domain.[32] The procedure consisted of heating the sample to 60°C and then, with $\mathbf{H}_c$ oriented along ⟨100⟩, cooling down to ~150°K by slowly pouring liquid nitrogen directly into the Dewar. The temperature was monitored with a copper-constant thermocouple soldered to one current lead of the sample. When the temperature of the sample reached 150°K, the magnetic field was reduced to zero and the sample cooled to 4.2°K. It is necessary to remove $\mathbf{H}_c$ at $T>120$°K to avoid the possibility of "domain flipping" (discussed in the Appendix).

A detailed investigation to determine the critical field needed to obtain a single domain was not carried out, but it was apparent that the critical field is determined by the condition of the sample. In a pure, relatively strain-free crystal (Cr 9), a single domain was obtained with $H_c=30$ kOe, whereas for some other crystals $H_c=150$ kOe was insufficient.

All data were taken at 4.2°K since it was determined experimentally that lowering the temperature to 1.2°K had a negligible effect on the galvanomagnetic properties. The data consist of two types: (1) voltage versus field direction at constant field strength (rotation diagrams) and (2) voltage versus field strength at constant field direction (field sweeps). The standard procedure of reversing both the magnetic field and the current was normally followed unless it was found that reversing the current gave no new information. The magnetoresistance was normalized in the usual manner, i.e.,

$$\Delta\rho/\rho\equiv[\rho(H)-\rho(0)]/\rho(0),$$

where $\rho(0)$ is the resistivity in zero magnetic field at 4.2°K, and $\rho(H)$ is the resistivity in a field H.

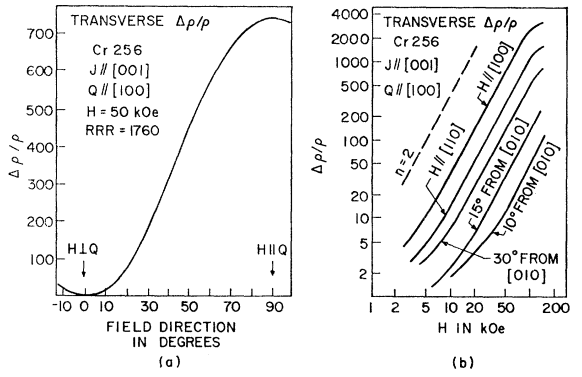

FIG. 4. (a) Rotation diagram of transverse magnetoresistance for J ∥ [001] and Q⊥J. (b) Field dependence of the transverse magnetoresistance for the Q and J directions of Fig. 4(a). Oscillations have been averaged out. Dashed line indicates slope= 2.0.

[32] Although an H_c of 150 kOe was used for most of the data, some data were taken for $H_c=205$ kOe.

V. EXPERIMENTAL RESULTS

In the measurements reported here, the current J was parallel to either [001] or [110]. Since Q can be successively oriented along each ⟨100⟩ axis, these two current directions are sufficient to obtain all the relevant data. In describing the data, we therefore specify the orientation of H, J, and Q with respect to the crystallographic axes.

With J along [001], H in the (001) plane, and Q⊥J, the transverse magnetoresistance exhibits twofold symmetry. A nearly sinusoidal rotation diagram [Fig. 4(a)] is obtained with a maximum of H ∥ Q and a minimum at H⊥Q. In some samples a cusp is observed for H ∥ Q and/or H⊥Q. We conclude from measurements on multidomain crystals that a residual cusp is indicative of an imperfect single domain (see Fig. 13).

With the exception of the case H⊥Q, the transverse $\Delta\rho/\rho$ increases without bound. However, in contrast to the LAK theory, the field dependence is not quadratic over the entire range of H. Figure 4(b) shows several log-log plots of $\Delta\rho/\rho$ versus H for Q⊥J. If we write $\Delta\rho/\rho=AH^n$, then for each field direction n varies from $n<1$ to $n\sim2.0$. "Ideal" quadratic behavior[33] is obtained roughly between 20 and 100 kOe, depending on orientation, with most values of n lying near 1.9 in this region. Above and below these field values n decreases continuously from 1.9. For some directions of H, an actual decrease in $\Delta\rho/\rho$ is observed at high fields.

In each case where n decreases from its maximum value at high fields, large-amplitude oscillations are observed which are periodic in $1/H$. Typical curves are shown in Fig. 5. For the curves of Fig. 4(b) the oscilla-

[33] By ideal quadratic behavior we mean $1.8\leq n\leq2.0$. Even in nontransition metals with no magnetic breakdown the exponent n lies in this range.

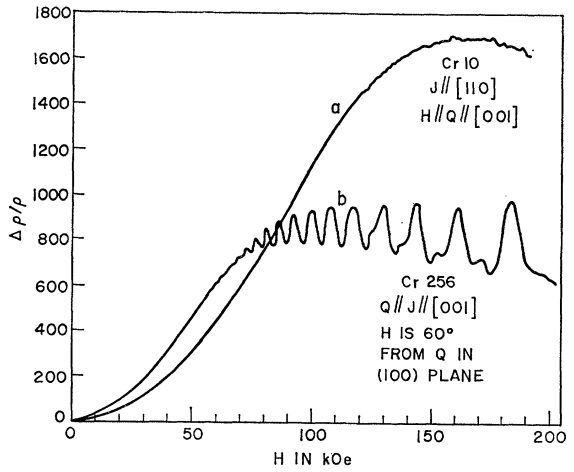

FIG. 5. Field dependence of magnetoresistance up to 200 kOe showing the oscillations.

tions have been averaged out. No oscillations are observed where $\Delta\rho/\rho$ increases quadratically, except for field directions within 15° of [010] in the (001) plane where **Q** || [100] and **J** || [001] [bottom two curves of Fig. 4(b)]. A more detailed study of the oscillatory magnetoresistance will be reported in a separate paper.[34]

At the minima in Fig. 4(a), and for all field directions in the plane perpendicular to **Q** when **Q**⊥**J**, $\Delta\rho/\rho$ saturates. The saturating field dependence of $\Delta\rho/\rho$ was difficult to reproduce from sample to sample and in some cases even a negative $\Delta\rho/\rho$ was observed [see Fig. 11(b)]. These results appear to depend on sample geometry and/or lead placement.

If in a sample with **J** || [001] the wave vector **Q** is oriented parallel to **J**, the data are fourfold symmetric as shown in the top curve of Fig. 6(a). A very large magnetoresistance that is sensitive to any tilting of **H** out of the transverse plane is obtained. To obtain the curve of Fig. 6(a) it was necessary to tilt **H** through the transverse plane at various angles and plot the sharp maxima (half-width ~3°) of the tilt curves. The dramatic effect of "reorienting" the tetragonal Fermi surface is shown in the lower curve of Fig. 6(a) where **Q**⊥**J** in the *same* sample. The measured values of RRR differ for the two Q directions since the residual zero-field resistivity increases by 37% when the direction of **Q** is changed from **Q**⊥**J** to **Q** || **J**.

Although $\Delta\rho/\rho$ obtains its largest values for **H**⊥**Q** and **Q** || **J**, quadratic dependence is never observed. For all orientations of **H** in the transverse plane n decreases slowly but continuously above and below ~30 kOe from a maximum value of $n=1.7$. Thus the two regions where n deviates from the theoretical value of 2.0 seem to merge. Two such curves are shown in Fig. 6(b) for the [100] and [110] minima in the rotation diagram. The oscillations have again been averaged out.

The results of measurements on a sample with **J** || [110] and **Q**⊥**J** are similar to those of Fig. 4. For **Q** || [100] or **Q** || [010], however, large peaks are observed in $\Delta\rho/\rho$ [Fig. 7(a)] for **H**⊥**Q**. The minima at **H** || [1$\bar{1}$0] are unequal for the two Q directions because of an unequal number of residual domains along [001] (an H_c of only 30 kOe was used in this experiment). A transverse-even voltage with large peaks for **H**⊥**Q** is also observed. In Fig. 7(b) the two mutually perpendicular transverse-even voltages V_{24} and V_{13} are shown separately for clarity. They reverse sign when the **Q** direction is changed from [100] to [010]. The small discontinuities in V_{13} at **H** || [1$\bar{1}$0] are again due to small residual domains along [001], since they are not observed when $H_c=150$ kOe. The residual zero-field resistivity increases by 25% when the **Q** direction is changed from [001] to either [100] or [010].

In Fig. 7(c) we show field sweeps for **J** || [110] and **Q** || [100]. While for **H**⊥**Q**, n is never larger than 1.5, it is apparent that the deviation from quadratic behavior at high fields is less drastic than for other orientations.

A rotation diagram of the Hall voltage is shown in Fig. 8 for **J** || [001] and **Q** || [100]. A sharp maximum is observed in the voltage at **H**⊥**Q**. The field dependence of the Hall voltage is nonlinear for the entire range of H. Again two distinct regions of anomalous behavior can be identified. In all cases the voltage is initially positive with a maximum at ~3 kOe (Fig. 9). Above 3 kOe the Hall voltage for **H**⊥**Q** remains positive [Fig. 9(a)] with a second maximum between ~30 and 50 kOe depending on the orientation of **H** in the plane perpendicular to **Q**. As the voltage crosses zero between ~50 and ~100 kOe, large oscillations are also observed.

For field directions more than 15° out of the plane perpendicular to **Q** the Hall voltage becomes negative at ~12 kOe. Between 20 and 40 kOe it is almost linear and extrapolates approximately to zero at zero field [Fig. 9(b)]. Above 40 kOe it decreases faster than linear with no evidence of oscillations. In Fig. 9(b) there is evidence that at the highest fields the curve is again tending toward linearity.

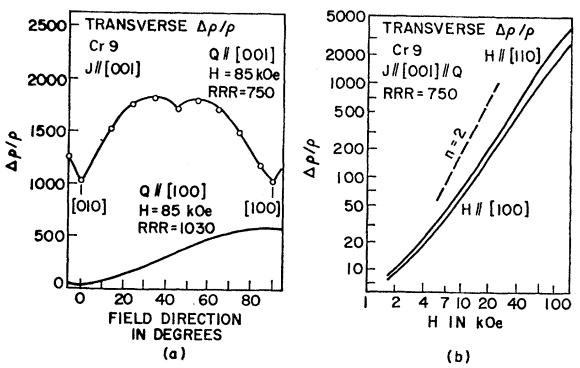

FIG. 6. (a) Rotation diagrams of transverse magnetoresistance for **Q** directions parallel and perpendicular to **J** in the same sample. (b) Field dependence of the transverse magnetoresistance for **Q** || **J**. Dashed line indicates slope =2.0.

[34] A. J. Arko, J. A. Marcus, and W. A. Reed (to be published).

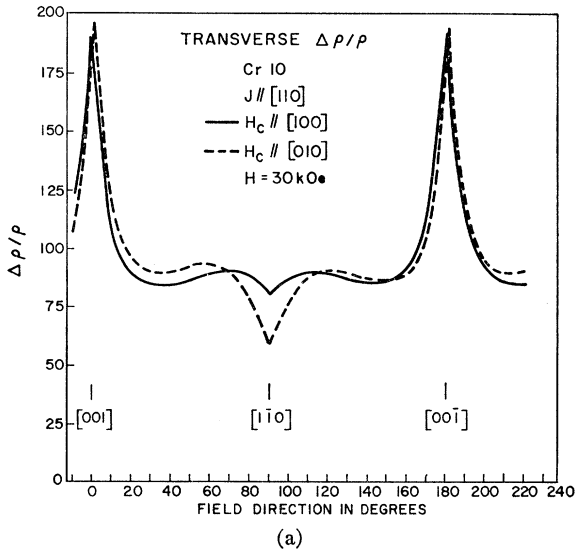

(a)

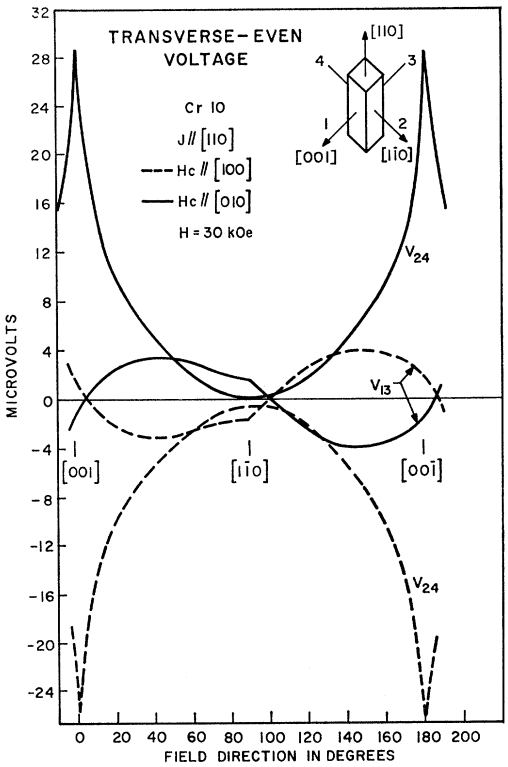

(b)

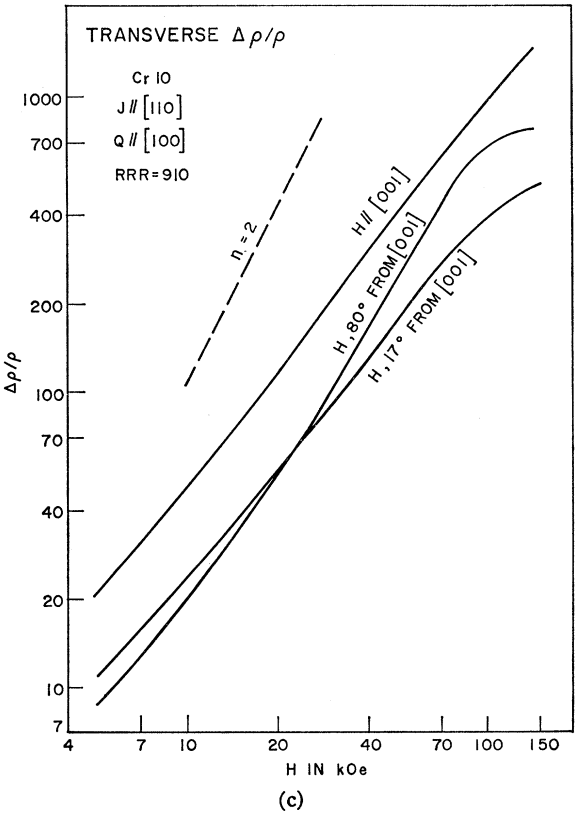

(c)

FIG. 7. (a) Rotation diagrams of transverse magnetoresistance for **J** || [110] and **Q** successively oriented along the two diagonal ⟨100⟩ directions. (b) Rotation diagrams of the transverse-even voltage for the two Q directions of Fig. 7(a). The voltages V_{24} and V_{13} were measured on probes as shown in the insert. (c) Field dependence of transverse magnetoresistance for **Q** along one of the diagonal directions. Oscillations have been averaged out. Dashed line indicates slope=2.0.

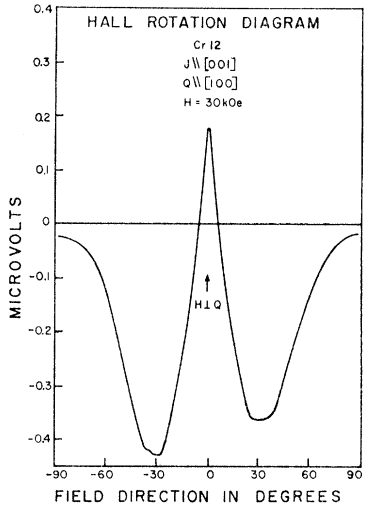

FIG. 8. Rotation diagram of the Hall voltage for $\mathbf{Q} \perp \mathbf{J}$, and $\mathbf{H}$ in the transverse plane.

Reduced Kohler diagrams for $\mathbf{Q} \perp \mathbf{J}$ are shown in Fig. 10. Subject to certain conditions[35] which are approximately satisfied in the high-field region in metals with no magnetic breakdown, the magnetoresistance from samples having different $\rho(0)$ should fall on one curve when plotted versus $H/\rho(0)$ (or RRR$\times H$, where RRR means the residual resistivity ratio). There should be no difference between varying $\rho(0)$ by impurities [Fig. 10(a)] or by temperature [Fig. 10(b)]. There is no doubt that above $\sim$100 kOe Cr does not obey Kohler's rule. At lower fields, however, there is some ambiguity. When $\rho(0)$ is changed by merely increasing the temperature in the same sample, small deviations are observed that are beyond experimental error. When data from samples of different RRR are plotted on a Kohler diagram, the deviations, if any, are hidden by the experimental errors arising from differences in domain perfection, misorientation, variation in lead attachment, etc.

The planar Hall voltage (i.e., the quadratic Hall voltage in the plane of $\mathbf{H}$ and $\mathbf{J}$) was not investigated in detail because of the limited information that it yields. The data obtained do, however, show the proper symmetry, with the field dependence generally reflecting the field dependence of $\Delta\rho/\rho$.[36]

A zero longitudinal magnetoresistive voltage ($V=0$, $\Delta\rho/\rho=-1$) was observed in some samples with $\mathbf{J} \parallel [001]$ and $\mathbf{Q} \perp \mathbf{J}$ from $\sim$20 to 150 kOe, the largest field for which data were obtained. It is believed to be a geometrical effect[37] due to the contact area of the current leads being small compared to the sample cross section. This, combined with the large anisotropy of the magnetoresistivity in the plane perpendicular to $\mathbf{J}$, results in a highly anisotropic current distribution so

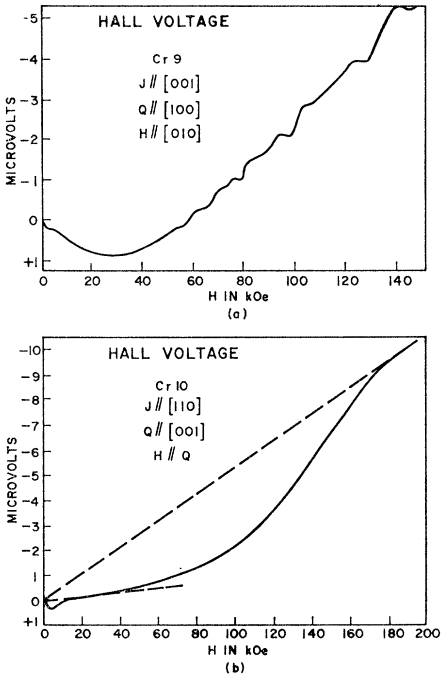

FIG. 9. Field dependence of the Hall voltage. Note that positive and negative axes of the ordinate are interchanged for easier comparison with Fig. 12. Negative values correspond to electron-like behavior. (a) $\mathbf{H} \perp \mathbf{Q}$. (b) $\mathbf{H} \parallel \mathbf{Q}$. Dashed lines indicate the assumed asymptotic behavior.

[35] The assumptions are (1) that collisions can be described by a relaxation time $\tau(\mathbf{k})$, and (2) that changes in temperature or purity alter all $\tau(\mathbf{k})$ by the same factor. (See Ref. 25 for a more detailed discussion.)

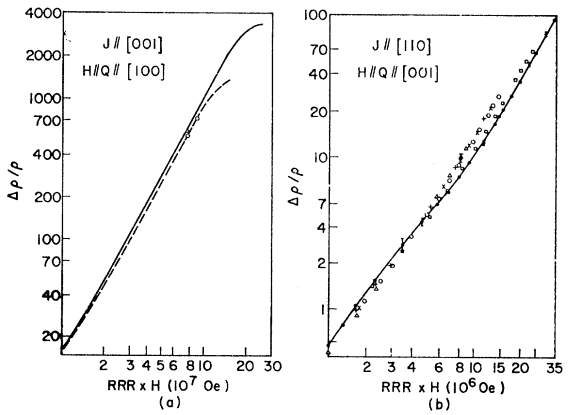

FIG. 10. Reduced Kohler diagrams for $\mathbf{H} \parallel \mathbf{Q}$. (a) Measurements at 4.2°K using different samples. Solid line: Cr 265 before cutting (RRR=1760); dashed line: Cr 9 (RRR=1030); □: Cr 256 after cutting (RRR=1800); △: Cr 260 first mounting (RRR=1560); ○: Cr 260 second mounting (RRR=1560). (b) Measurements on Cr 10 at various temperatures. Solid line: RRR=1140 (4.2°K); □: RRR=840; ○: RRR=480; ×: RRR=384; +: RRR=341; △: RRR=296. Typical error bars are shown at various points.

[36] More complete data on the planar-Hall effect can be found in A. J. Arko, Ph.D. thesis, Northwestern University (unpublished). The sign of the Hall voltage as reported in the thesis is reversed.

[37] N. E. Alexeevskii, N. B. Brandt, and T. I. Kostina, Zh. Eksperim. i Teor. Fiz. **34**, 1339 (1958) [English transl.: Soviet Phys.—JETP **7**, 924 (1958)].

that $V=0$ is a consequence of $\mathbf{J}=0$ in the region of the potential leads. Measurements from two pairs of potential leads attached on mutually perpendicular $\langle 100\rangle$ corners of the sample showed that the anomalous voltages are observed on the pair attached in the plane of $\mathbf{Q}$ and $\mathbf{J}$, while normal saturation of $\Delta\rho/\rho$ is observed on the pair in the plane perpendicular to the $\mathbf{Q}$-$\mathbf{J}$ plane (see Fig. 11). The effect of anisotropy is demonstrated by changing the $\mathbf{Q}$ direction through 90° in the (001) plane. The voltages observed on the two pairs of potential leads are interchanged after the reorientation of $\mathbf{Q}$ so that a zero voltage is again observed on the pair in the $\mathbf{Q}$-$\mathbf{J}$ plane. Although a zero longitudinal magnetoresisitive voltage has been observed for a limited range of fields in other metals,[38,39] the ability to reorient the Fermi surface in Cr without changing the sample geometry makes this the ideal metal for studying geometrical effects. A detailed discussion will appear in a separate publication.[22]

VI. DISCUSSION OF RESULTS

A. Topological Features of the Fermi Surface of Cr

The LAK theory predicts that in the high-field limit $\Delta\rho/\rho$ should either saturate or increase quadratically with increasing field. It is apparent that large deviations from this ideal behavior are observed in Cr. We will defer until Sec. VI B the discussion of the deviations associated with changes in topology and the degree of compensation resulting from magnetic breakdown.

Since for all magnetic field directions which do not allow open orbits the magnetoresistance increases "nearly quadratically," we conclude that Cr is a compensated metal ($n_e=n_h$). This result is expected since Cr has an even atomic number and one atom per unit cell.

The saturation of $\Delta\rho/\rho$ for $\mathbf{H}$ in the plane perpendicular to $\mathbf{Q}$ when $\mathbf{Q}\perp\mathbf{J}$ and $J\parallel[001]$ indicates a sheet (or sheets) of open orbits topologically similar to a cylinder with its axis in the $\mathbf{Q}$ direction. The open orbits are also reflected in the Hall voltage, which shows a sharp spike as $\mathbf{H}$ is rotated through the point $\mathbf{H}\perp\mathbf{Q}$. The failure to observe any additional discontinuities in the rotation diagrams of both $\Delta\rho/\rho$ and the Hall voltage for $\mathbf{H}$ in the transverse plane with $\mathbf{Q}\perp\mathbf{J}$ and $\mathbf{J}\parallel[001]$ enables us to rule out the possibility of any additional open-orbit directions except possibly along [001]. Open orbits in this direction can be ruled out from data on a sample with $\mathbf{J}\parallel[110]$ and $\mathbf{Q}\parallel[001]$, since no discontinuity is observed in either $\Delta\rho/\rho$ or the Hall voltage for $\mathbf{H}\parallel\mathbf{Q}$. They are also ruled out by symmetry.

For $\mathbf{Q}\parallel\mathbf{J}$ the field dependence of transverse $\Delta\rho/\rho$ is "nearly quadratic," as expected for open orbits along $\mathbf{J}$. This is the case even for $\mathbf{H}\parallel\langle 100\rangle$ where minima are observed in the rotation diagram. The failure to observe

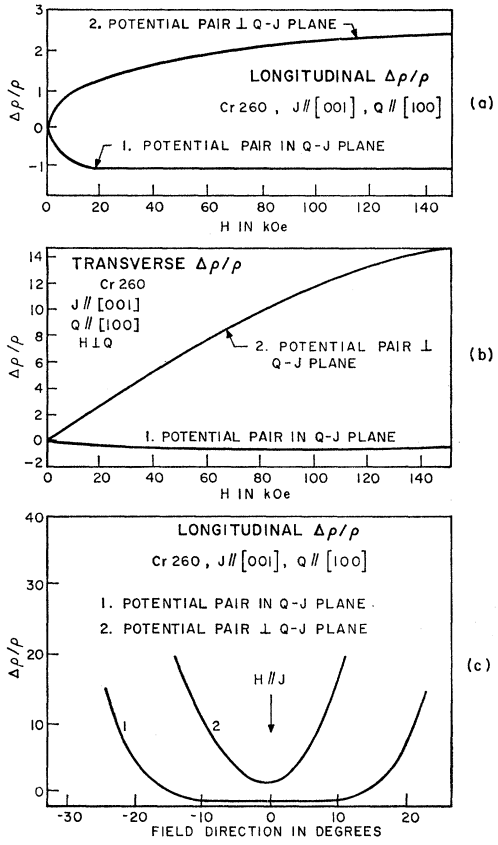

FIG. 11. Magnetoresistance measured on two potential pairs placed on two mutually perpendicular corners of a crystal with $\mathbf{J}\parallel[001]$, $\mathbf{H}\perp\mathbf{Q}$ and $\mathbf{Q}\perp\mathbf{J}$. (a) Longitudinal field dependence. (b) Transverse field dependence. (c) Rotation diagram with $H=100$ kOe rotated in the $\mathbf{Q}$-$\mathbf{J}$ plane.

saturation for these orientations indicates that the minima are not due to additional open orbits.

The most unambiguous determination of the open direction is obtained in a sample with $\mathbf{J}\parallel[110]$, $\mathbf{Q}\parallel[100]$ (or [010]), and $\mathbf{H}$ in the transverse plane. Any open orbits will appear as peaks or minima in the transverse-even voltage. Since the small discontinuity in V_{13} shown in Fig. 7(b) was not observed in a perfect single domain the only peaks that need to be considered occur at $\mathbf{H}\parallel[001]$. The angle between $\mathbf{J}$ and the open-orbit directions, α, was determined from the equations in Table I and found to be $\pm 45°\pm 2°$ for $\mathbf{Q}\parallel[100]$ and $\mathbf{Q}\parallel[010]$, respectively.

The nearly sinusiodal rotation diagram for $\mathbf{J}\parallel[001]$ and $\mathbf{Q}\parallel[100]$ implies that any undulations on the cylindrical sheet must be small compared to the cylinder diameter.[40]

The data are in excellent agreement with the model discussed in Sec. II. This model has several sets of open orbits all of which are directed along $\mathbf{Q}$. Although several of these open orbits are contorted and would

[38] Kunihide Tanaka, Sci. Rept. Res. Inst. Tohoku Univ. **16**, 123 (1964).
[39] J. Yahia and J. A. Marcus (unpublished).
[40] W. A. Reed, E. Fawcett, and R. R. Soden, Phys. Rev. **139**, A1557 (1965).

themselves probably cause a sharp minimum in $\Delta\rho/\rho$ at $\mathbf{H}\perp\mathbf{Q}$, the relatively large and smooth cylindrical sheets dominate the magnetoresistance.

The large anisotropy of the zero-field resistivity parallel ($\rho_{||}$) and perpendicular ($\rho_\perp$) to $\mathbf{Q}$ is presumed to be due to the anisotropic truncation of the Fermi surface by the spin-density wave.[3] If to a first approximation we assume a constant electron mass and velocity over each sheet of the Fermi surface, then the ratio $\rho_\perp/\rho_{||}=1/1.37$ indicates that there are $\sim 27\%$ fewer carriers contributing to $\rho_{||}$ than to $\rho_\perp$. Although this is in qualitative agreement with the model, the complexity of the Fermi surface and the large number of energy gaps make quantitative comparisons impossible.

The *topology* of the Fermi surface of antiferromagnetic Cr as proposed by Lomer is consistent with our data. It must remain for such investigations as the dHvA effect, however, to verify the details.

B. Effects of Magnetic Breakdown

Magnetic breakdown through the superlattice energy gaps in Cr was first predicted by Lomer,[1] though he made no attempt to estimate H_n, the breakdown field corresponding to nth-order energy gaps. Falicov and Zuckermann[2] found that the calculated value of H_n depends sensitively on the assumptions made about the energy bands. If we assume a first-order energy gap of 0.14 eV as determined from optical measurements by Barker *et al.*,[41] H_1 varies from 240 to 5400 kOe depending on whether the bands are nearly free-electron-like, d-like, or hybridized s- and d-like. For these same assumptions the values of H_2 lie approximately between 0.1 and 12 kOe, while all values of H_3 are of the order 1 Oe or less. On the basis of these calculations, it appears likely that the deviations in our data from ideal behavior at low fields are due to breakdown through second-order energy gaps, while at high fields the deviations are due to first-order gap breakdown. However, the experimental evidence is insufficient to allow a unique assignment of the order of the energy gaps to specific breakdown regions.

For the following reasons there is little doubt that magnetic breakdown occurs at high fields: (1) The large deviation from H^2 dependence in $\Delta\rho/\rho$ for all orientations indicates that either the topology or the degree of compensation is changing; (2) large-amplitude oscillations, periodic in $1/H$, are always observed in association with these deviations; and (3) Kohler's rule is not obeyed at high fields.

It is not as clear that the effects at low fields are due to magnetic breakdown. Similar deviations from H^2 dependence in $\Delta\rho/\rho$ could arise from a failure to achieve the high-field limit for certain pieces of the Fermi surface that have a large m^* (e.g., those with d-like character, or the large cylindrical pieces). Until these pieces achieve the high-field limit, Cr could behave as an uncompensated metal similar to the case observed[40] in Re. On the basis of the model used to explain the Re data, however, the Hall voltage is not expected to reverse sign as it does in Cr, although it would certainly be nonlinear. The change in sign of the Hall voltage is the most convincing evidence for magnetic breakdown in Cr at low fields. In addition, the slight deviations from Kohler's rule at low fields, at least where $\rho(0)$ is changed by increasing the temperature, are suggestive of magnetic breakdown. Falicov and Sievert[21] have shown that in complete magnetic breakdown the scattering process is described by an effective relaxation time, τ_{eff}, given by

$$1/\tau_{\text{eff}}=(1/\tau)+C\omega_n, \tag{6}$$

where τ is the relaxation time with no magnetic breakdown, C is a constant of order unity, and ω_n is the cyclotron frequency at the breakdown field H_n. Since $\rho(0)$ is not directly propoertional to $1/\tau_{\text{eff}}$, Kohler's rule is not obeyed.

By itself the Kohler plot [Fig. 10(b)] is inconclusive, particularly since data from samples of different RRR are not consistent with data from one sample at different temperatures. Conceivably, an anisotropic temperature-dependent magnetic disorder scattering could cause similar effects. When considered in conjunction with other evidence, however, the departure from Kohler's rule strengthens the breakdown hypothesis.

The details of magnetic breakdown at low fields cannot be determined from our data. There is a possibility that Cr is uncompensated at low fields, but another possibility is that smaller orbitals are merging into larger ones, together with a decrease in the relaxation time.

The nature of the breakdown at high fields is somewhat better understood. The data show that magnetic breakdown occurs for all orientations of the field. If for $H\ll H_1$ the metal is compensated with one direction of open orbits, then only four types of orbits coupled by magnetic breakdown can result in the tendency toward saturation of $\Delta\rho/\rho$ at high fields: (1) closed orbits breaking down to open orbits perpendicular to $\mathbf{J}$; (2) closed orbits breaking down to several open orbits with two or more arbitrary open directions; (3) closed orbits of one type breaking down to closed orbits of another type, causing the net number of holes and electrons to be unequal (uncompensated); and (4) open orbits that make an angle $\alpha<90°$ with $\mathbf{J}$ breaking down to closed orbits, causing the metal to become uncompensated.

If the breakdown mechanism is that of (1) or (2), then when breakdown is complete, the Fermi surface must be open in all directions, which seems topologically impossible.

The data are consistent with (3) and (4) if we assume that only a small number of orbits are breaking down. For case (3) even a very small number of hole

[41] A. S. Barker, Jr., B. I. Halperin, and T. M. Rice, Phys. Rev. Letters **20**, 384 (1968).

orbits breaking down to electron orbits (or vice versa) will have large effects on $\Delta\rho/\rho$. For case (4), however, a small number of open orbits breaking down to closed orbits would result in only small deviations from H^2 dependence in $\Delta\rho/\rho$ regardless of the resulting state of compensation.

From the sign of the Hall voltage, we conclude that magnetic breakdown results in an excess Δn of electrons. When magnetic breakdown is complete, we can define the Hall constant for a given direction of H as $R=\Omega/\Delta nec$, where Ω is the volume of the unit cell. If we assume that the dashed line in Fig. 9(b) reasonably approximates the asymptotic behavior of the Hall voltage, then for $\mathbf{H} \parallel \mathbf{Q}$ we have $\Delta n=0.17$ electrons per unit cell. A search has been made to find pieces of the Fermi surface in Fig. 3 where a transition from hole to electron orbits is possible. Since none is found, we conclude that some part of the hole surface located at H must remain when Cr beomes antiferromagnetic, and it is the breakdown of orbits on this surface to orbits on the electron surface at X_1, or the remaining surface at Γ which causes saturation and oscillations in $\Delta\rho/\rho$.

The magnitude of the energy gaps can be calculated from an estimate of the breakdown fields. Because of the complexity of the Fermi surface and the large number of gaps where breakdown is possible, H_n obtained from galvanomagnetic data is at best some average value. It is likely that for each orientation of H there exists a spectrum of energy gaps for all orders. Thus, Trego and Mackintosh[42] concluded from their measurements of the resistivity anomaly at T_N that first-order gaps vary in magnitude from 0.08 to 0.14 eV. Such a variation in Δ_n again arises from differences in the electronic energy bands[2] that are affected in varying degrees by the lattice and superlattice potentials.

A calculation to determine H_n has not been attempted because the pieces of the Fermi surface and the energy gaps undergoing breakdown have not been identified. We can, however, make estimates of H_n by comparing the data to the theoretical curves of Falicov and Sievert (Fig. 12) calculated on the basis of circular (free-electron) orbits. It appears from their curves[21] that when magnetic breakdown results in a change in the sign of the Hall voltage, the crossing point is less than or equal to the breakdown field. The estimate of the breakdown field obtained in this way is probably correct to within an order of magnitude in all cases. As an example, a typical curve is shown in Fig. 12(b) for hole orbits breaking down to electron orbits where the crossing point corresponds exactly to the breakdown field. Applying this criterion to our Hall data, we estimate that $H_2\sim 10$ kOe.

To calculate Δ_2 we use Eq. (5). Assuming free-electron-like bands and $v_\perp\approx v_{||}$, we can write

$$\Delta_n\approx[H_nE_Fe\hbar/m^*c]^{1/2}, \quad (7)$$

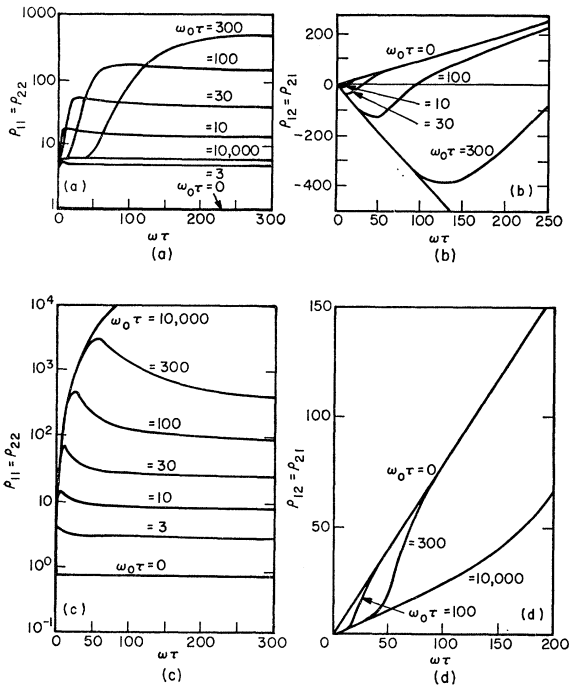

FIG. 12. Theoretical curves of galvanomagnetic effects in metals with magnetic breakdown taken from Falicov and Sievert (Ref. 21). ω_0 is the cyclotron frequency at the breakdown field H_0. (a) Magnetoresistivity for a transition from a closed hole orbit to a closed electron orbit in a cubic system. (b) Hall resistivity for the same transition. (c) Magnetoresistivity for a transition from closed compensated orbits to closed electron orbits in a cubic system. (d) Hall resistivity for the latter transition.

where $E_F=\frac{1}{2}[m^*(v_F)^2]$. Using 7 eV for the Fermi energy E_F, we get $\Delta_2=0.03$ eV. It is implied in the theory of Falicov and Zuckermann that for this case $\Delta_1=(2E_F\Delta_2)^{1/2}$ so that $\Delta_1=0.65$ eV. These are anomalously high values, and H_2 would have to be decreased by an unlikely factor of 10^3 in order to obtain a Δ_1 in agreement with the experimentally determined value. It is apparent that the free-electron velocity cannot be used in our calculations.

For hybridized s- and d-like bands, a much better determination of the electron velocity is obtained from the tight-bonding approximation. Falicov and Zuckermann found that H_n can be approximated by

$$H_n\approx(32\hbar c/ea^2)(\Delta_n/\Delta_{\mathrm{BW}})^2=2.5\times10^9(\Delta_n/E_{\mathrm{BW}})^2, \quad (8)$$

where E_{BW} is the bandwidth. Taking $E_{\mathrm{BW}}=3$ eV, a more realistic value of 0.006 eV is obtained for Δ_2. The relationship between Δ_1 and Δ_n in the same approximation is

$$\Delta_n\approx\Delta_1(\Delta_1/E_{\mathrm{BW}})^{n-1}, \quad (9)$$

so that Δ_1 as found from H_2 is 0.13 eV. This is in good agreement with the values determined from optical and resistivity anomaly measurements, considering the approximate nature of the calculations.

[42] A. L. Trego and A. R. Mackintosh, Phys. Rev. 166, 495 (1968).

To obtain an estimate of H_1 from the data, we again make use of the theoretical curves of Falicov and Sievert. Figures 12(c) and 12(d) are the magnetoresistivity and Hall resistivity for the transition from closed compensated orbits to closed electron orbits. The Hall resistivity becomes linear at $\omega\tau \approx \frac{1}{8}\omega_0\tau$. Since in Fig. 9(b) it appears that for $\mathbf{H} \parallel \mathbf{Q}$ the Hall voltage becomes linear at $\sim$200 kOe, we estimate H_1 for this orientation to be $\sim$600 kOe. A slightly higher estimate ($H_1 \sim 700$ kOe) is obtained from the peak in the magnetoresistivity that is observed at 160 kOe for $\mathbf{H} \parallel \mathbf{Q}$. If we choose H_1 to be 650 kOe, a reasonable estimate of the error is 20%. The energy gap then is $\sim$0.25 eV when calculated in the free-electron approxition and $\sim$0.05 eV in the tight-binding approximation. For $\mathbf{H} \perp \mathbf{Q}$ the breakdown field is somewhat lower judging from the onset of oscillations at $\sim$50 kOe as opposed to 100 kOe for $\mathbf{H} \parallel \mathbf{Q}$.

The value of 0.05 eV determined from the tight-binding approximation is in reasonable agreement with the minimum first-order gap of 0.08 eV observed by Trego and Mackintosh. The free-electron approximation, on the other hand, consistently yields values that are far too large. Since the Fermi surface of Cr is not expected to be free-electron-like, this result is not surprising. Our results then are consistent with other measurements if we assume that only the smallest first-order gaps are breaking down at 200 kOe, and that the electron velocity can be obtained from the tight-binding approximation.

We must also consider the possibility that our assignment of the order of the gaps is in error. In an attempt to fit some dHvA frequencies to the Lomer model of the Fermi surface, Graebner and Marcus[43] found no evidence for breakdown of second-order gaps up to 32 kOe, the limit of their measurements. If the spin-density wave contains harmonics, the higher-order energy gaps and the corresponding H_n would be much larger than the values predicted by Falicov and Zuckermann. Thus we cannot discount the possibility that at high fields we are actually observing second-order gap breakdown.

VII. CONCLUSIONS

The Fermi surface of antiferromagnetic Cr consists of several sheets, at least one of which is open along $\mathbf{Q}$ and is topologically similar to a cylinder. This is consistent with the Lomer model of the Fermi surface where the open orbits are a result of energy gaps introduced in the energy spectrum by the spin-density wave. The direction of open orbits can be oriented along any $\langle 100 \rangle$ axis by appropriately cooling Cr through T_N in a large magnetic field.

Deviations from ideal behavior of the galvanomagnetic effects at high fields ($H > 100$ kOe) are attributed to magnetic breakdown through first-order energy gaps. Where only closed orbits exist the breakdown most probably results in noncompensation. For $\mathbf{H} \parallel \mathbf{Q}$ breakdown results in an excess of 0.17 electrons per unit cell. For $H < 20$ kOe the deviations from ideal behavior are tentatively attributed to magnetic breakdown through second-order energy gaps. For values of H where no magnetic breakdown is evident, Cr is a compensated metal.

The estimates of the breakdown fields are $\sim$650 kOe for first-order gaps and $\sim$10 kOe for second-order gaps. In order to obtain from our breakdown fields energy gaps in reasonable agreement with other experiments, it is necessary to assume hybridized s- and d-like electron bands. There is probably a spectrum of first-order gaps, and only the smallest ones ($\Delta_1 \approx 0.05$ eV) are breaking down in fields up to 200 kOe.

ACKNOWLEDGMENTS

The authors wish to thank the staff at the Francis Bitter National Magnet Laboratory for the use of their facilities, and in particular L. G. Rubin who has been most helpful and cooperative. Numerous discussions with L. M. Falicov and M. J. Zuckermann have proven invaluable in the interpretation of some data. Extensive exchanges of information and helpful discussions with J. E. Graebner and R. M. Montalvo are also greatly appreciated. We also wish to thank G. F. Brennert for technical assistance.

APPENDIX: MEASUREMENTS ON MULTIDOMAIN SAMPLES

A relatively uniform distribution of domains with their $\mathbf{Q}$'s along the three $\langle 100 \rangle$ directions results in

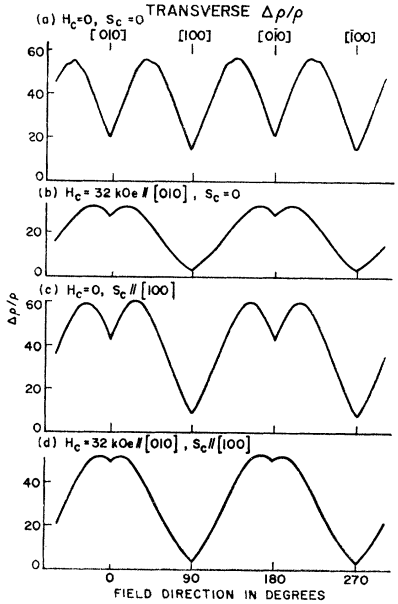

FIG. 13. Rotation diagrams of transverse magnetoresistance in multidomain samples. H_c and S_c are the magnetic field and compressive stress applied during cooling through T_N.

[43] J. E. Graebner and J. A. Marcus (to be published).

rotation diagrams with cubic symmetry. An example is shown in Fig. 13(a) for $\mathbf{J} \parallel [001]$. The small notches at [110] are because of the domains along [001]. The minima at ⟨100⟩ are sharp rather than round as in the single domain, presumably because of the domains along [001]. A sinusoidal rotation diagram with four-fold symmetry is obtained when only two types of domains with $\mathbf{Q} \perp \mathbf{J}$ exist in the cystal.

Figure 13(b) shows the result of cooling in a field not large enough to produce a single domain. (A single domain is assumed to be characterized by the absence of a minimum in the direction of $\mathbf{H}_c$.) Heating the crystal above T_N erases all effects of field cooling, while cooling with $\mathbf{H}_c$ along the perpendicular direction induces entirely similar effects displaced by 90°.

The effect of a compressive stress $\mathbf{S}_c$ applied while cooling through T_N [Fig. 13(c)], was reported[44] in a preliminary paper on Cr. It was shown later by neutron diffraction[17] that $\mathbf{S}_c$ promotes the growth of the two domains with $\mathbf{Q} \perp \mathbf{S}_c$. This is the case in Fig 13(c) where a few kg/mm^2 are as effective as $H_c = 30$ kOe. By simultaneously applying $\mathbf{H}_c$ along [010] and $\mathbf{S}_c$ along [100] the formation of a single domain along [010] is enhanced as seen in Fig. 13(d). This is a useful way of obtaining single domains when only small fields are available. The drawbacks are that only one or at most two pairs of potential leads can be attached, and a permanent strain can be induced in the specimen, which is not erased by heating above T_N.

The preference of the domains to orient along the ⟨100⟩ directions perpendicular to the compressive stress can be qualitatively understood on the basis of the experiments of McWhan *et al.*[45] who have shown that hydrostatic pressure decreases the energy gap and hence the strength of the antiferromagnetic interaction. If a uniaxial compression decreases the energy gap for domains along the compression axis, it becomes energetically more favorable for domains to orient along the perpendicular axes.

Another interesting phenomenon is that of "domain flipping." It stems from the preference of electron spins in an antiferromagnet to align perpendicular to $\mathbf{H}$. A

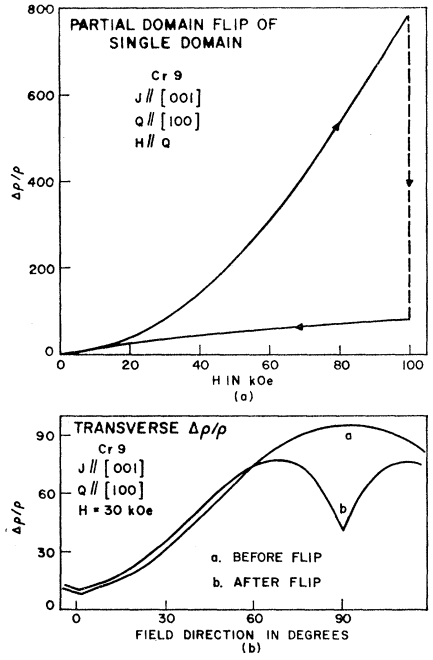

FIG. 14. (a) Example of a partial domain flip in a single-domain sample caused by reversing the sample current at 100 kOe. The initial portion of the curve up to 100 kOe is reproducible if the sample is undisturbed. (b) Rotation diagrams of transverse magnetoresistance before and after the domain flip of part a.

sufficiently large field oriented along $\mathbf{Q}$ below $T_F = 120$°K, where the spin-density wave is longitudinally polarized, will tend to reorient or "flip" the domains in directions perpendicular to $\mathbf{H}$. When this happens there is a sudden drop in $\Delta\rho/\rho$ because of the appearance of open orbits perpendicular to $\mathbf{H}$. If the specimen is not completely a single domain, the flipping will occur at fields as low as 30–40 kOe. A complete single domain, however, is stable to $H > 100$ kOe before it starts to flip. The actual value varies from sample to sample but in all samples with $\mathbf{J} \parallel [110]$ and $\mathbf{Q} \parallel [001]$ the domains were stable to 150 kOe. If a large $\mathbf{H}$ ($\sim$100 kOe) is applied along $\mathbf{Q}$ and the sample current is abruptly reversed, the domain will suddenly flip [Fig. 14(a)] presumably because of the added energy of mechanical vibration. In multidomain specimens vibration of the sample rod at low fields was sufficient to cause domain flipping. Figure 14(b) shows the rotation diagrams of Cr 9 before and after the domain flip of Fig. 14(a).

[44] A. J. Arko and J. A. Marcus, in *Proceedings of the Ninth International Conference on Low-Temperature Physics, Columbus, Ohio* (Plenum Press, Inc., New York, 1965), p. 748.

[45] D. B. McWhan and T. M. Rice, Phys. Rev. Letters **19**, 846 (1967).